

Enhanced calcification ameliorates the negative effects of UV radiation on photosynthesis in the calcifying phytoplankter *Emiliana huxleyi*

GUAN WanChun^{1,3} & GAO KunShan^{2*}

¹ College of Life Science, South China Normal University, Guangzhou 510631, China

² State Key Laboratory of Marine Environmental Science, Xiamen University, Xiamen 361005, China

³ Department of Marine Science, School of life sciences, Wenzhou Medical College, Wenzhou, 325035, China

Received June 23, 2009; accepted September 25, 2009

The calcifying phytoplankton species, coccolithophores, have their calcified coccoliths around the cells, however, their physiological roles are still unknown. Here, we hypothesized that the coccoliths may play a certain role in reducing solar UV radiation (UVR, 280–400 nm) and protect the cells from being harmed. Cells of *Emiliana huxleyi* with different thicknesses of the coccoliths were obtained by culturing them at different levels of dissolved inorganic carbon and their photophysiological responses to UVR were investigated. Although increased dissolved inorganic carbon decreased the specific growth rate, the increased coccolith thickness significantly ameliorated the photoinhibition of PSII photochemical efficiency caused by UVR. Increase by 91% in the coccolith thickness led to 35% increase of the PSII yield and 22% decrease of the photoinhibition of the effective quantum yield (Φ_{PSII}) by UVR. The coccolith cover reduced more UVA (320–400 nm) than UVB (280–315 nm), leading to less inhibition per energy at the UV-A band.

BWF, coccolith, dissolved inorganic carbon, *Emiliana huxleyi*, photochemical efficiency, UVR

Citation: Guan W C, Gao K S. Enhanced calcification ameliorates the negative effects of UV radiation on photosynthesis in the calcifying phytoplankter *Emiliana huxleyi*. Chinese Sci Bull, 2010, 55: 588–593, doi: 10.1007/s11434-010-0042-5

More than one third of the anthropogenic CO₂ released to the atmosphere since the industrial revolution has been absorbed by the oceans [1]. Increased dissolution of CO₂ into seawater increases concentrations of pCO₂, HCO₃⁻ and H⁺ and decreases CO₃²⁻ levels and saturation state of calcium carbonate [2]. Therefore, the oceanic surface waters have already been acidified by 0.1 pH units (corresponding to a 30% increase of H⁺) since 1800 and will further decrease by another 0.3–0.4 units (about 100%–150% increase of H⁺) by 2100 under a “business-as-usual” emission scenario [3,4]. This ongoing ocean acidification at such magnitude and pace has not occurred in the past 300 million years [4]. Chemical changes in the seawater carbonate system due to ocean acidification have been shown to harm marine calci-

fyng organisms by reducing the rate of calcification of their skeletons or shells [5,6].

Coccolithophores calcify and produce coccoliths intracellularly, which are expelled and displayed around the cells. They perform two kinds of carbon fixation, photosynthesis and calcification, therefore, play an important role in biogeochemical cycles of CO₂ [7]. *Emiliana huxleyi* (Prymnesiophyceae) is a representative species of coccolithophores, often found in many coastal and open oceans [8]. Formation of coccoliths (diameter, 2–4 μm) of *E. huxleyi* cells is known to be affected by many environmental factors. Studies showed that *E. huxleyi* cells are resistant to high levels of PAR, showing negligible photoinhibition [9]. It was assumed that the coccoliths may help dissipate high solar radiation [7]. However, other studies showed later on that the photoinhibition-tolerance of this organism was in-

*Corresponding author (email: ksgao@xmu.edu.cn)

dependent of coccoliths [10,11] and calcification was not supposed to have a protective role in dissipating energy under high levels of PAR [12]. However, it is unknown whether the coccoliths can shield off UV irradiances.

Solar UVB (280–315 nm) is known as a natural stress factor for phytoplankton [13]. Depletion of ozone caused by industrial activities has caused increased UV-B irradiance reaching the earth's surface [13]. Although the enhanced rate of chloride in stratosphere has slowed down since the Montreal Protocol, the recovery time of the ozone layer is delayed due to the effect of global warming that leads to further cooling in the stratosphere [14]. Solar UVB is known to damage DNA and proteins of phytoplankton [15,16], alter cyanobacterial morphology [17], and reduce photosynthetic activity [18] and nutrient uptake [19]. Growth of *E. huxleyi* is sensitive to UV-B [20–22], however, little is known about its photosynthetic performance and the relation with the coccolith cover when exposed to UV. Consequently, this study aims to investigate the photosynthetic responses of *E. huxleyi* to solar UVR and to get insight into whether the thicker coccoliths would decrease the deleterious effect of UVR.

1 Materials and methods

1.1 Species and culture conditions

Emiliania huxleyi (CS-369) was obtained from CSIRO (Commonwealth Scientific and Industrial Research Organization, Australia) and maintained in the K media [23], under cool-white fluorescent light at about $50 \mu\text{mol photons m}^{-2} \text{s}^{-1}$ (12L:12D) and 20°C in a growth chamber (GXZ-300D, China). The cells were allowed to acclimate to $400 \mu\text{mol m}^{-2} \text{s}^{-1}$ of PAR gradually (the initial phase: cells were exposed to $50 \mu\text{mol m}^{-2} \text{s}^{-1}$ for 4 d, the middle phase: the culture was refreshed and then exposed to $200 \mu\text{mol m}^{-2} \text{s}^{-1}$ for 4 d, and the third phase: the culture was refreshed again, then exposed to $400 \mu\text{mol m}^{-2} \text{s}^{-1}$). Before being used for experiments, they had been grown at $500 \mu\text{mol m}^{-2} \text{s}^{-1}$ of PAR for 8 generations for them to acclimate to the experimental PAR level. Cells at the exponential phase (3.5×10^6 cells mL^{-1}) were diluted to 0.5×10^6 cells mL^{-1} with the K media before being used for the experiments. For the UV-exposures, incubations were carried out in quartz tubes (2 cm in diameter, 7 cm long), which were maintained in a water bath for temperature control ($20 \pm 0.5^\circ\text{C}$) using a cooling circulator (CAP-3000, Rikakikai, Tokyo, Japan).

1.2 Experimentation

The experiments were carried out at the Marine Biology Institute, Shantou University, in May, 2007. Photosynthetic carbon fixation, photochemical efficiency (Φ_{PSII}), and particulate inorganic carbon (PIC) content per cell were meas-

ured. Biological weighted function (BWF) was established to distinguish the effects of different UV wavelengths on photosynthesis in the cells with different thicknesses of coccoliths.

1.3 Enrichment of dissolved inorganic carbon (DIC) in media

Sodium bicarbonate was used to raise the concentrations of DIC in the filtrated and sterilized seawater enriched with K medium. The concentration of DIC for the media without adding sodium bicarbonate was 2 mmol/L (seawater DIC level). The enriched levels of DIC were 7 and 22 mmol/L. The levels of pH of the media were 8.05, 8.15 and 8.25 for the low, intermediate and high DIC levels, respectively. The cells were collected and re-suspended in the fresh K media of 2 mmol/L DIC for the investigation on their response to UVR.

1.4 Measurement of particulate inorganic carbon (PIC)

The amount of particulate inorganic carbon (PIC) was estimated according to Takano et al. [24]. Briefly, the total inorganic carbon concentration (IC_1) of the *E. huxleyi* cultures was determined using a total organic carbon analyzer (TOC-5000, Shimadzu Corp., Kyoto, Japan). IC_1 includes both the inorganic carbon of the PIC (coccoliths) and the dissolved inorganic carbon (DIC) in the growth medium. Then, the inorganic carbon concentration (IC_2) of the filtrate (Whatman GF/F) was also determined. The PIC content was derived as the difference between IC_1 and IC_2 . Since *E. huxleyi* does not possess an efficient CO_2 concentrating mechanism [25,26], the influence of the intracellular inorganic carbon pool on the estimation of PIC was neglected.

1.5 Solar radiation monitoring and radiation treatments

Incident solar radiation was continuously monitored using a broadband ELDONET filter radiometer (Real Time Computer, Möhrendorf, Germany) which has 3 channels for photosynthetically active radiation (PAR, 400–700 nm), ultraviolet-A (UVA, 315–400 nm) and ultraviolet-B radiation (UVB, 280–315 nm), respectively [27]. This device has been universally recognized (certificate No. 2006/BB14/1) [27,28] and was calibrated regularly with the assistance from the maker every year.

The cells were exposed to the following radiation treatments with or without UVR (UVA+B) or UVA: 1) PAB (PAR+UVA+B), tubes covered with a 295 nm cut-off foil (Ultraplan, Digepra, Munich, Germany), transmitting irradiances above 295 nm; 2) PA (PAR+UVA), tubes covered with 320 nm cut-off foil (Montagefolie, Folex, Dreieich, Germany), transmitting irradiances above 320 nm; and 3) P

(PAR), tubes covered with a-395 nm cut-off foil (Ultraplan UV Opak, Digefra, Munich, Germany), transmitting irradiances above 395 nm. The transmission spectra of these foils are available elsewhere [29].

1.6 Measurements of photosynthesis

The cells of stable physiological performance (grown at $500 \mu\text{mol m}^{-2} \text{s}^{-1}$ for 8 generations at the exponential phase) were used for measurements of photosynthesis. Each sample of 20 mL was inoculated with 50 μL of 5 μCi (0.185 MBq) of labeled sodium bicarbonate (ICN Radiochemicals). After the incubations, cells were filtered onto a Whatman GF/F glass fiber filter (25 mm), which was then placed in a 20 mL scintillation vial, exposed to HCl fumes overnight, and dried at 45°C . The radioactivity of the fixed ^{14}C was counted with a scintillation counter (LS 6500 Multi-Purpose Scintillation Counter, Beckman Coulter, USA) after the filter was digested in the cocktail (Wallac Optiphase HiSafe 3, PerkinElmer life and Analytical Sciences, USA). The rate of photosynthetic carbon fixation was calculated according to Steeman [30].

1.7 Biological weighting functions (BWF)

For determination of the energy-dependant responses to UVR (BWF, biological weighting function) of photosynthesis, 6 different radiation treatments were carried out using the cut-off filters (Schott) that cut the solar radiation at 280, 295, 305, 320, 350, and 395 nm (the transmission spectra of these filters have been published elsewhere, Villafañe et al. [31]). The incubations lasted 3 h for the determination of the BWF. The irradiances of PAR, UVA and UVB for the BWF exposures were 298.1, 45.5 and 1.4 W m^{-2} , respectively. The BWF curves were obtained by using the BWF-PI model [32]. The mean energy between each pair of filter intervals was calculated using the STAR software [33] with the data recorded by the ELDONET spectroradiometer. An exponential decay function (base 10) was used to fit the data in each experiment, and the exponent of the function was expressed as a third-degree polynomial function, the best fit was obtained by iteration ($R^2 > 0.95$).

1.8 Determination of photochemical efficiency

The effective quantum yield (Φ_{PSII}) was measured with a pulse-amplitude-modulated fluorometer (PAM-WATER-ED, Walz, Germany) according to Genty et al. [34] as follows: $\Phi_{\text{PSII}} = \Delta F/F'_m = (F'_m - F_t)/F'_m$, where F'_m represents the instant maximal fluorescence and F_t the steady state fluorescence of light-adapted cells. The saturating light pulse was $5300 \mu\text{mol m}^{-2} \text{s}^{-1}$ with 0.8 s duration. Measuring light is about $0.3 \mu\text{mol m}^{-2} \text{s}^{-1}$, and the actinic light $10 \mu\text{mol m}^{-2} \text{s}^{-1}$.

Inhibition of Φ_{PSII} was calculated as: $\text{Inh} (\%) = (Y_P - Y_{\text{UVR}}) \times Y_P^{-1} \times 100$, where Y_P indicates the yield of the sample under PAR, while Y_{UVR} indicates the yield for samples exposed to either PAR+UVA or PAR+UVA+B.

1.9 Cell size and growth rates

The cells were examined with a Carl Zeiss microscope (AxioPlan 2, Germany) and their sizes were measured using an Axiovision software. The specific growth rate (μ) was determined as follows: $\mu = \ln(C_a/C_b)/(t_a - t_b)$, where C_a and C_b are the cell concentrations (cells mL^{-1}) on day a and b, respectively. Sizes of the cells with or without coccoliths were also assessed with a flow cytometer (BD FACSAria, USA), using FSC-A to reflect the unicellular diameter. The cells without coccoliths (naked-cells) were obtained by sparging pure CO_2 into the media for 30 s [35].

1.10 Data analysis and statistics

A one-way analysis of variance (ANOVA) and *t*-test were used to determine significant difference among the radiation treatments. A confidence level was set at $P=0.05$.

2 Results

The specific growth rate of *E. huxleyi* was significantly lower under the elevated levels of DIC, being reduced by 27% at 7 mmol/L and by 14% at 22 mmol/L DIC (Figure 1). However, the size of the cells either with or without the coccolith increased with the enrichment of DIC (Figure 2). When the DIC was raised from 2 to 22 Mm, the cells with the diameter bigger than $9 \mu\text{m}$ increased from 2% to 66% (Figure 2(b)). The FSC-A by flow cytometer, indicating the cell size, also evidenced the increment in the cell size, by

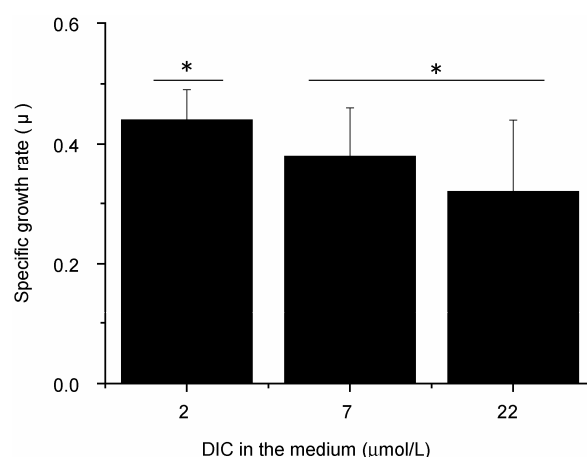


Figure 1 The specific growth rate on day 6 of *Emiliania huxleyi* in batch cultures with different DIC levels (2, 7, and 22 mmol/L) during the long-term period (from Mar 19th to 29th, 2007). * indicates significance ($P < 0.05$).

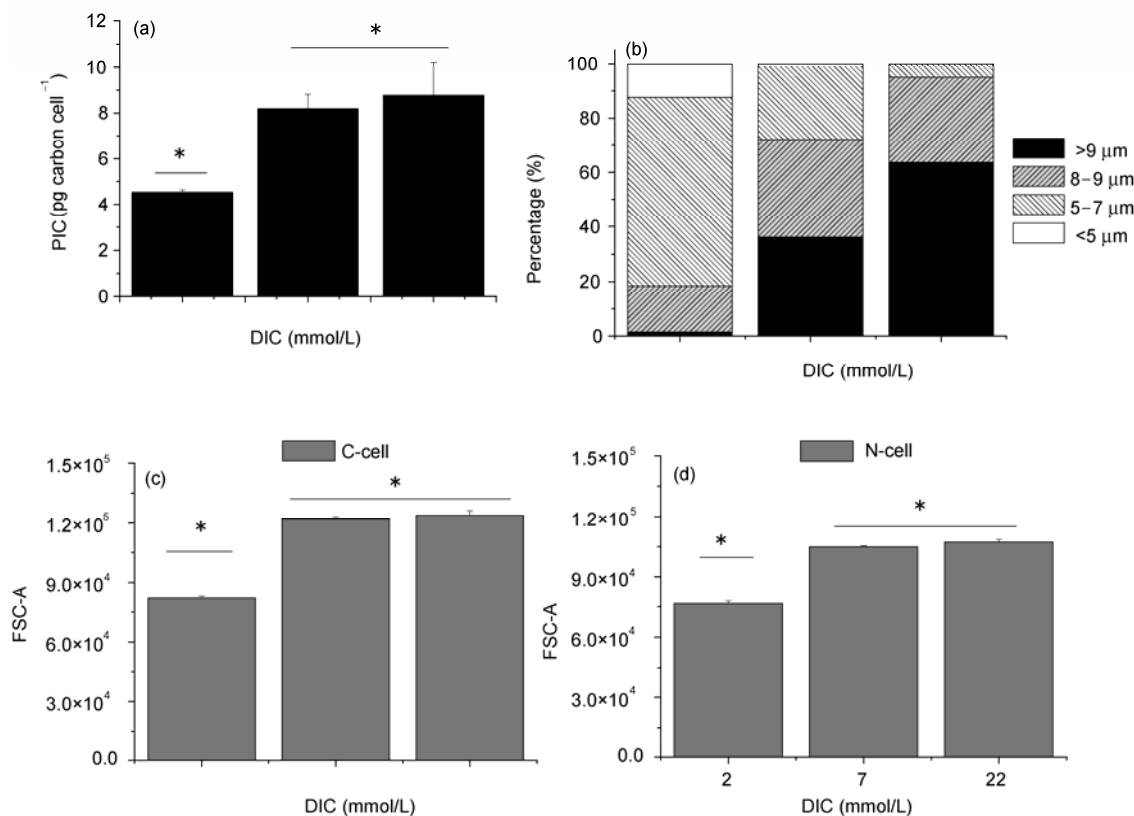


Figure 2 The particulate inorganic carbon contents (PIC) (a), cell size measured by a microscope (b), and FSC-A measured by a flow cytometer (c, d) of *Emiliania huxleyi* grown at different DIC levels (2,7 and 22 mmol/L) for 6 d (Mar 19–25, 2007). The asterisks indicate the significant difference ($P < 0.05$).

about 40%, with the enrichment of DIC (Figure 2(c) and (d)). The thickness of coccoliths or the PIC content increased by 81% at 7 mmol/L and by 91% at 22 mmol/L compared with that of the control. There was no significant difference between 7 and 22 mmol/L DIC for both PIC content and cell size (FSC-A) (Figure 2(a), (c) and (d)) ($P > 0.05$). The PIC amount per cell surface area was increased from 0.3 (control, 2 mmol/L DIC) to about 0.4 pg carbon μm^{-2} (enriched DIC levels).

When the cells with different levels of PIC were exposed to UVR or UVR+PAR, they showed significant differences in the photochemical response to UV. The cells with higher levels of coccoliths were more tolerant to high PAR levels or UVR than the cells with less coccoliths (Figure 3). Compared with the control (2 mmol/L DIC), the yield increased by 9%, 13%, and 17% when the cells grown at 7 mmol/L DIC were exposed to PAR, PAR+UVA, and PAR+UVR, respectively. The yield increased correspondingly by 9%, 33%, and 35% for the cells grown at 22 mmol/L DIC (Figure 3(a)). The inhibition of the photochemical yield was significantly down-regulated in the cells with a thicker coccolith cover. The cells with different PIC or coccolith thickness showed significant difference in the sensitivity to different wavebands of UVR, as reflected by the BWF (Figure 4). Photosynthetic carbon fixation rate of the cells with a thicker coccolith cover was less inhibited by the UVA

band of 320–380 nm. The ratio of the inhibition with the thicker coccoliths to that with the thinner coccoliths was 0.29 for the UVA band of 320–380 nm, while it was 3.44 for the UVB band of 285–310 nm.

3 Discussion

Decreased growth rates under DIC-enriched conditions may be attributed to: (1) The reduced energy supply for growth due to the enhanced energy requirement for calcification; (2) the thicker coccoliths around the cells decreased the energy for photosynthesis. Therefore, the lower cell division and the higher calcification rate led to the larger cells (Figure 2). The enhanced calcification and subsequently the increased amount of coccoliths were probably due to the increased state of calcium carbonate saturation.

The cells with thicker coccoliths are more tolerant of high levels of PAR and UVR in view of the photosynthetic performance (Figure 3). Recently, coccolith has been found to reduce the transmission of PAR and UVR by 10%–22% and 20%–25%, respectively [35]. The present study showed that increased coccoliths led to less photosynthetic inhibition caused by UV (Figure 3). This is consistent with the finding that reduced coverage of the coccoliths under seawater acidified conditions led to enhanced photosynthetic

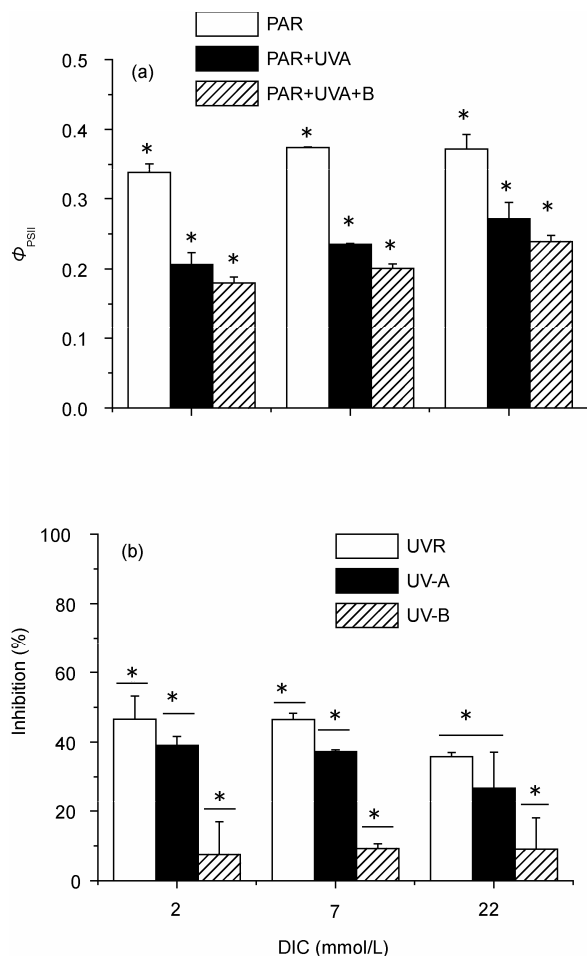


Figure 3 The difference in effective quantum yield (a) of the *Emiliania huxleyi* cells exposed to PAR (395–700 nm), PAR+UVA (320–700 nm) and PAR+UVA+B (295–700 nm) for 60 min, and UVR-induced inhibition (b). *E. huxleyi* cells were grown at different DIC levels (2, 7 and 22 mmol/L) for 6 d (Mar 19–25, 2007) ($n = 4$). The mean irradiances of solar radiation in 1 h (Mar 25, 2007, 10: 20–11: 20) were 270.41 (PAR, 400–700 nm), 40.77 (UVA, 315–400 nm), and 1.28 (UVB, 280–315 nm) $W m^{-2}$. The asterisks mean the significant difference ($P < 0.05$).

inhibition caused by UV in *E. huxleyi* [35].

Studies showed that the growth rate of *E. huxleyi* was decreased by UVB at only one tenth of its common incident biological effective dose ($100 J m^{-2} d^{-1}$) [36], and even halted at higher levels of UVB (above $400 J m^{-2} d^{-1}$) [20]. Such inhibition of growth induced by UVR was relative to DNA damage [20,36,37]. Its cell size and contents of photoprotective pigments were also found to increase after the cells had been exposed to UVR [20,21,37]. Under high levels of PAR, *E. huxleyi* can adjust its photosynthetic performance by either altering its effective absorption cross-sections or altering its photosynthetic unit (PSU) size [38]. In the present study, *E. huxleyi* cells grown at the enriched DIC levels became bigger and more tolerant of UVA (320–380 nm) (Figure 2). Our recent finding showed that the coccolith screened more UV-A than UV-B [35]. A higher percentage of attenuated UVA due to the increased light

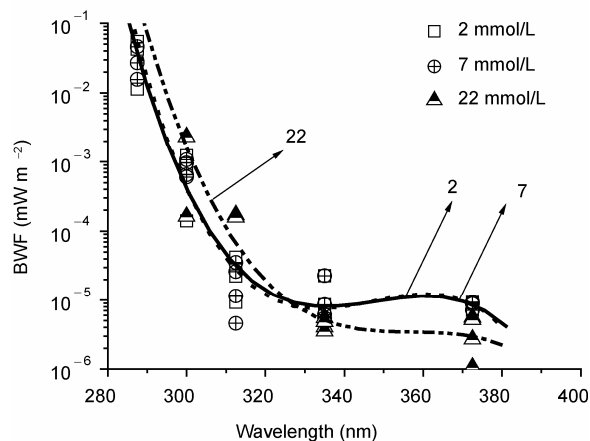


Figure 4 The difference in biological weighting function (BWF) for cells grown at different DIC levels (2, 7 and 22 mmol/L) for 6 d (Mar 19th to 25th, 2007) ($n = 3-6$). The mean irradiances of solar radiation over the incubation period (Mar 25, 2007, 11:00–12:00) were 298.11 (PAR, 400–700 nm), 45.51 (UVA, 315–400 nm), and 1.41 (UVB, 280–315 nm) $W m^{-2}$. The DIC level for measuring BWF was about 2 mmol/L.

path associated with increased coccolith thickness and cell size could lead to reduction of the harms caused by UV-A. Therefore, the larger cells with thicker coccoliths had the longer path for UVR to reach the nuclei, so less DNA was damaged and less harm was caused to PSII. The difference in the UV-related inhibition between the cells grown in 7 and 22 mM DIC was probably due to the difference in cell size, which was significantly larger at the enriched DIC level.

In the oceanic waters, coccolithophores calcify to different degrees due to chemical and physical differences at different geographical sites [39]. *E. huxleyi* is known to be distributed within <30 m of depth and its maximal cell density is often found at 10–20 m depth [10,39–42]. The cells within 20 m are often exposed to UV-A as well as UV-B [43–45]. Therefore, the cells can be affected by UV while they are mixed up and down. On the other hand, the ongoing ocean acidification, leading to changes in seawater carbonate chemistry, will decrease the thickness of the coccoliths [35], and will definitely affect the photophysiological responses of *E. huxleyi* to solar UVR.

This work was supported by the National Basic Research Program of China (Grant No. 2009CB421207), National Natural Science Foundation of China (Grant Nos. 40930846 and 40676063) and MEL Young Scientist Visiting Fellowship of State Key Laboratory of Marine Environment Science, Xiamen University and Ph.D. Foundation of Wenzhou Medical College (Grant Nos. MELRS0935 and 89209008).

- 1 Sabine C L, Feely R A, Gruber N, et al. The oceanic sink for anthropogenic CO_2 . *Science*, 2004, 305: 367–371
- 2 Feely R A, Sabine C L, Lee K, et al. Impact of anthropogenic CO_2 on the $CaCO_3$ system in the oceans. *Science*, 2004, 305: 362–366
- 3 Brewer P G. Ocean chemistry of the fossil fuel CO_2 signal: the haline signal of “business as usual”. *Geophys Res Lett*, 1997, 24: 1367–1369

- 4 Caldeira K, Wickett M E. Anthropogenic carbon and ocean pH. *Nature*, 2003, 425: 365
- 5 Gao K S, Aruga Y, Asada K, et al. Calcification in the articulated coralline alga *Corallina pilulifera*, with special reference to the effect of elevated CO₂ concentration. *Mar Biol*, 1993, 117: 129–132
- 6 Riebesell U, Zondervan I, Rost B, et al. Reduced calcification of marine plankton in response to increased atmospheric CO₂. *Nature*, 2000, 407: 364–367
- 7 Paasche E. A review of the coccolithophorid *Emiliana huxleyi* (Prymnesiophyceae), with particular reference to growth coccolith formation, and calcification-photosynthesis interactions. *Phycologia*, 2001, 40: 503–529
- 8 Holligan P M, Fernandez E, Aiken J, et al. A biogeochemical study of the coccolithophore, *Emiliana huxleyi*, in the North Atlantic. *Glob Biogeochem Cycl*, 1993, 7: 879–900
- 9 Nielsen M V. Growth, dark respiration and photosynthetic parameters of the coccolithophorid *Emiliana huxleyi* (Prymnesiophyceae) acclimated to different day length-irradiance combinations. *J Phycol*, 1997, 33: 818–822
- 10 Nanninga H J, Tyrell T. Importance of light for the formation of algal blooms by *Emiliana huxleyi*. *Mar Ecol Prog Ser*, 1996, 136: 195–203
- 11 Harris G N, Scanlan J S, Geider R J. Acclimation of *Emiliana huxleyi* (Prymnesiophyceae) to photon flux density. *J Phycol*, 2005, 41: 851–862
- 12 Trimborn S, Langer G, Rost B. Effect of varying calcium concentrations and light intensities on calcification and photosynthesis in *Emiliana huxleyi*. *Limnol Oceanogr*, 2007, 52: 2285–2293
- 13 Häder D P, Kumar H D, Smith R C, et al. Effect of solar UV radiation on aquatic ecosystems and interactions with climate change. *Photochem Photobiol*, 2007, 6: 267–285
- 14 Weatherhead E C, Andersen S B. The search of the signs of recovery of ozone layer. *Nature*, 2006, 441: 39–45
- 15 Boelen P, De-Boer M K, Kraay G W, et al. UVBR-induced DNA damage in natural marine picoplankton assemblages in the tropical Atlantic Ocean. *Mar Ecol Prog Ser*, 2000, 193: 1–9
- 16 Xiong F S. Evidence that UV-B tolerance of the photosynthetic apparatus in microalgae is related to the D1-turnover mediated repair cycle *in vivo*. *J Plant Physiol*, 2001, 158: 285–294
- 17 Wu H Y, Gao K S, Villafañe V E, et al. Effects of solar UV radiation on morphology and photosynthesis of filamentous cyanobacterium *Arthrospira platensis*. *Appl Environ Microb*, 2005, 71: 5004–5013
- 18 Guan W C, Gao K S. Light histories influence the impacts of solar ultraviolet radiation on photosynthesis and growth in a marine diatom, *Skeletonema costatum*. *J Photochem Photobiol B Biol*, 2008, 91: 151–156
- 19 Behrenfeld M J, Hardy J T, Lee H II. Ultraviolet-B radiation effects on inorganic nitrogen uptake by natural assemblages of oceanic phytoplankton. *J Phycol*, 1995, 31: 25–36
- 20 Buma A G J, van Oijen T, van de Poll W. The sensitivity of *Emiliana huxleyi* (Prymnesiophyceae) to ultraviolet-B radiation. *J Phycol*, 2000, 36: 296–303
- 21 Van Rijssel M, Buma A G J. UV radiation induced stress does not affect DMSP synthesis in the marine prymnesiophyte *Emiliana huxleyi*. *Aquat Microb Ecol*, 2002, 28: 167–174
- 22 Guan W C, Gao K S. Impacts of UV radiation on photosynthesis and growth of the coccolithophore *Emiliana huxleyi* (Haptophyceae). *Environ Exp Bot*, 2010, 67: 502–508
- 23 Keller M D, Selvin R C, Claus W, et al. Media for the culture of oceanic ultraplankton. *J Phycol*, 1987, 23: 633–638
- 24 Takano H, Takei R, Manabe E, et al. Increased coccolith production by *Emiliana huxleyi* cultures enriched with dissolved inorganic carbon. *Appl Microbiol Biotechnol*, 1995, 43: 460–465
- 25 Raven J A, Johnston A M. Mechanisms of inorganic carbon acquisition in marine phytoplankton and their implications for the use of other resources. *Limnol Oceanogr*, 1991, 36: 1701–1714
- 26 Nimer N A, Merrett M J. Calcification and utilization of inorganic carbon by the coccolithophorid *Emiliana huxleyi* Lohmann. *New Phytol*, 1992, 121: 173–177
- 27 Häder D P, Lebert M, Marangoni R, et al. ELDONET - European light dosimeter network hardware and software. *J Photochem Photobiol B Biol*, 1999, 52: 51–58
- 28 Korbee-Peinado N, Abdala-Díaz R T, Figueroa F L, et al. Ammonium and UV radiation stimulate the accumulation of mycosporine-like amino acids in *Porphyrha columbina* (Rhodophyta) from patagonia, argentina. *J Phycol*, 2004, 40: 248–259
- 29 Zheng Y Q, Gao K S. Impacts of solar UV radiation on the photosynthesis, growth, and UV-absorbing compounds in *Gracilaria lemaneiformis* (Rhodophyta) grown at different nitrate concentrations. *J Phycol*, 2009, 45: 314–323
- 30 Steeman N E. The use of radio-active carbon (C¹⁴) for measuring organic production in the sea. *J Cons Perm Int Explor Mer*, 1952, 18: 117–140
- 31 Villafañe V E, Sundbäck K, Figueroa F L, et al. Photosynthesis in the aquatic environment as affected by UVR. In: Helbling E W, Zagarese H E, eds. *UV Effects in Aquatic Organisms and Ecosystems*. Cambridge: The Royal Society of Chemistry, 2003. 357–397
- 32 Neale P J, Kieber D J. Assessing biological and chemical effects of UV in the marine environment: Spectral weighting functions. In: Hester R E, Harrison R M, eds. *Causes and Environmental Implications of Increased UV-B radiation*. Cambridge: The Royal Society of Chemistry, 2000. 61–83
- 33 Ruggaber A, Dlugi R, Nakajima T. Modelling of radiation quantities and photolysis frequencies in the troposphere. *J Atmos Chem*, 1994, 18: 171–210
- 34 Genty B E, Briantais J M, Baker N R. Relative quantum efficiencies of the two photosystems of leaves in photorespiratory and non-photorespiratory conditions. *Plant Physiol Biochem*, 1989, 28: 1–10
- 35 Gao K S, Ruan Z X, Villafañe V E, et al. Ocean acidification exacerbates the effect of UV radiation on the calcifying phytoplankter *Emiliana huxleyi*. *Limnol Oceanogr*, 2009, 54: 1855–1962
- 36 Gieskes W W C, Buma A G J. UV damage to plant life in a photobiologically dynamic environment: the case of marine phytoplankton. *Plant Ecol*, 1997, 128: 17–25
- 37 Garde K, Caroline C. The impact of UV-B radiation and different PAR intensities on growth, uptake of ¹⁴C, excretion of DOC, cell volume, and pigmentation in the marine prymnesiophyte, *Emiliana huxleyi*. *J Exp Mar Biol Ecol*, 2000, 247: 99–112
- 38 Suggestt D, Le Floc H E, Harris G N, et al. Different strategies of photoacclimation by two strains of *Emiliana huxleyi* (Haptophyta). *J Phycol*, 2007, 43: 1209–1222
- 39 Balch W M, Holligan P M, Ackleson S G, et al. Biological and optical properties of mesoscale coccolithophore blooms in the Gulf of Maine. *Limnol. Oceanogr*, 1991, 36: 629–643
- 40 Ziveri P, Thunell R C. Coccolithophore export production in Guaymas Basin, Gulf of California: response to climate forcing. *Deep-Sea Res II*, 2000, 47: 2073–2100
- 41 Tyrrell T, Taylor A H. A modelling study of *Emiliana huxleyi* in the NE Atlantic. *J Mar Syst*, 1996, 9: 83–112
- 42 Robertson J E, Robinson C, Turner D R, et al. The impact of a coccolithophore bloom on oceanic carbon uptake in the northeast Atlantic during summer 1991. *Deep-Sea Res*, 1994, 41: 297–314
- 43 Boelen P, Obermosterer I, Vink A A, et al. Attenuation of biologically effective UV radiation in tropical Atlantic waters measured with a biochemical DNA dosimeter. *Photochem Photobiol*, 1999, 69: 34–40
- 44 Smith R C, Prezelin B B, Baker K S, et al. Ozone depletion: ultraviolet radiation and phytoplankton biology in Antarctic waters. *Science*, 1992, 255: 952–959
- 45 Gieskes W W C, Karry G W. Transmission of ultraviolet light in the Weddell Sea: report on the first measurements made in Antarctic. *Biomass Newsl*, 1990, 12: 12–14